Double Z-Pinch Hohlraum Drive with Excellent Temperature Balance for Symmetric Inertial Confinement Fusion Capsule Implosions

M. E. Cuneo,[1,*] R. A. Vesey,[1] J. L. Porter, Jr.,[1] G. R. Bennett,[2] D. L. Hanson,[1] L. E. Ruggles,[1] W. W. Simpson,[1] G. C. Idzorek,[3] W. A. Stygar,[1] J. H. Hammer,[4] J. J. Seamen,[2] J. A. Torres,[1] J. S. McGurn,[1] and R. M. Green[1]

[1]*Sandia National Laboratory, P.O. Box 5800, Albuquerque, New Mexico 87185-1193*

[2]*Ktech Corporation, 2201 Buena Vista S.E., Suite 400, Albuquerque, New Mexico 87106-4265*

[3]*Los Alamos National Laboratory, Los Alamos, New Mexico 87545*

[4]*Lawrence Livermore National Laboratory, P.O. Box 808, Livermore, California 94551*

(Received 28 January 2002; published 13 May 2002)

A double Z pinch driving a cylindrical secondary hohlraum from each end has been developed which can indirectly drive intertial confinement fusion capsule implosions with time-averaged radiation fields uniform to 2%–4%. 2D time-dependent view factor and 2D radiation hydrodynamic simulations using the measured primary hohlraum temperatures show that capsule convergence ratios of at least 10 with average distortions from sphericity of $\langle \Delta r \rangle / r \leq 30\%$ are possible on the Z accelerator and may meet radiation symmetry requirements for scaling to fusion yields of >200 MJ.

DOI: 10.1103/PhysRevLett.88.215004 PACS numbers: 52.59.Qy, 52.57.Fg, 52.58.Lq

Achieving inertial confinement fusion (ICF) in the laboratory has been a goal of the U.S. fusion program for the last 25 years [1]. High spherical convergence ratio ($C_r \geq 30$) implosions of fusion capsules containing frozen deuterium-tritium (DT) fuel theoretically allow ignition with the minimum driver energy by igniting a "hot spot" at the center of compressed cold fuel [1]. Implosion velocities $\geq$30 cm/μsec uniform to 1%, hot spot temperatures $\geq$5 keV, hot spot fuel areal densities $\geq$0.3 g/cm^2, and fuel preheat <1 eV are required to ignite and efficiently burn the DT fuel using indirect drive by soft x-ray sources [1]. Meeting these and other conditions places extremely challenging requirements on radiation temperature, symmetry, and pulse shape, and the capsule preheat produced by the driver [1]. Radiation symmetry may well be the most difficult requirement. A nearly spherical capsule $C_r \geq 30$ requires a time-integrated soft x-ray intensity variation $\langle \Delta I \rangle / I$ uniform within 1%–2% over the capsule surface consistent with distortions from spherical compression $\langle \Delta r \rangle / r \leq 25\%–50\%$ [1]. Recently z-pinch soft x-ray sources on the Z accelerator [2] have shown great potential as efficient ($\geq$10% wall plug) and low capital cost ($50–$100 per radiated joule) indirect drivers for inertial confinement fusion (ICF) implosions [3–7]. In particular, Z-pinch sources may be an excellent match to the capsule drive energies (1–2 MJ), radiation pulse lengths (5–20 ns), and characteristic hohlraum sizes (15–20 mm) necessary to implode the larger diameter fusion capsules ($\geq$5 mm) required for high fusion yields ($\geq$200 MJ), if the other driver requirements can be met [3,5–7]. High yield systems are critical for future fusion energy applications. In this Letter we demonstrate for the first time on a pulsed-power driven system, a double-Z-pinch soft x-ray source that drives a cylindrical secondary hohlraum from both ends and permits control of the capsule radiation-drive symmetry to levels of near term interest for ICF implosions ($\langle \Delta I \rangle / I = 2–4\%$). Time-resolved measurements of the pinch x-ray power and primary hohlraum temperatures show good balance between the upper and lower sources on a significant fraction of the shots. 2D radiation hydrodynamics (2D-RHD) simulations of capsule implosions were performed using the calculated time-dependent capsule radiation drive symmetry based on these measurements. These indicate that a capsule C_r of at least 10 is possible on the Z accelerator at a 70 eV drive temperature, with average distortions from sphericity of $\langle \Delta r \rangle / r \leq 30\%$. This performance would scale to a distortion $\langle \Delta r \rangle / r \leq 34\%$ at $C_r \approx 30$ at a high yield temperature of 220 eV, within the range for capsule ignition and burn [1], when the improved radiation symmetry resulting from the increase in wall albedo is taken into account. These predictions will be tested in x-ray backlit capsule implosion experiments [8].

In the double-Z-pinch configuration (Fig. 1A), a Z-pinch driven primary hohlraum is located at each end of a coaxial secondary hohlraum. The implosion and stagnation on axis of a 20-mm-diam by 10-mm-long wire array consisting of 300, 11.5 μm diam tungsten wires heats each primary hohlraum [6,7]. The two wire arrays are driven in series from a single electrical power feed at the base of the lower array. Beryllium radial spokes and axial shine shields at the secondary radiation entrance holes isolate the capsule from pinch plasma, magnetic field (current flow), and a direct view of the pinch at stagnation, allowing efficient radiation flow into the secondary hohlraum [3,6,7]. This configuration provides a highly effective approach to control of symmetry for a Z-pinch driven system [3,9]. Overlapping primary and secondary wall re-emission onto the capsule creates a radiation drive with a uniformity that depends on the primary and secondary geometry [9–11] and provides radiation smoothing over mm-scale-length pinch nonuniformities [3]. A cylindrically symmetric radiation drive can be conveniently represented in terms of Legendre polynomials. A 2D time dependent view factor or radiosity code called OPTSEC was

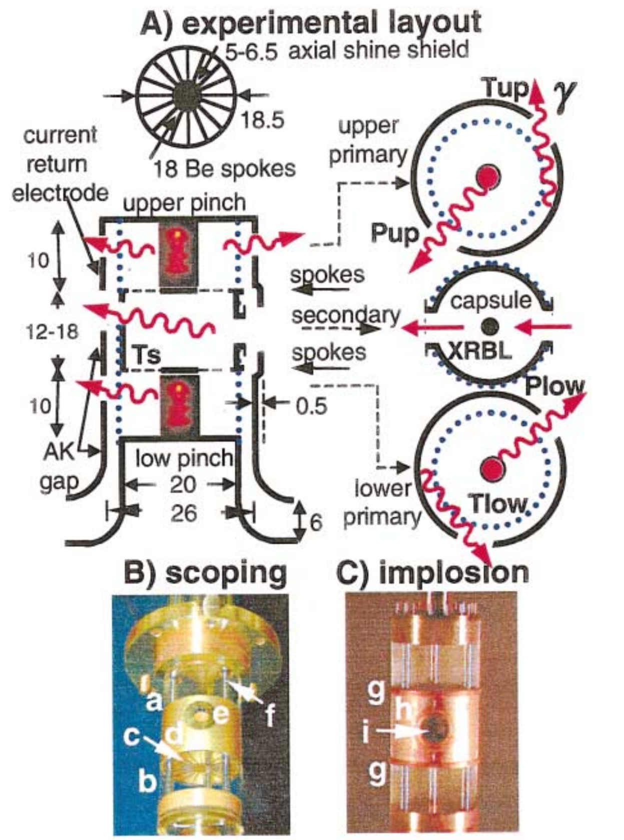

FIG. 1 (color). Double pinch geometry showing: (A) experimental and diagnostic LOS layout, (B) load for scoping studies, (C) load for implosion studies with (*a*) upper wire array, (*b*) lower wire array, (*c*) lower Be spokes and shine shield, (*d*) secondary, (*e*) aperture and tamping ring for secondary temperature measurement, (*f*) support rods removed prior to shot, (*g*) wire alignment slots, (*h*) raised aperture with wire holding ring, (*i*) x-ray backlighter (XRBL) LOS. The array is shown in the initial position in blue, diagnostic LOS shown in red. All dimensions in mm. The external primary hohlraum or current return electrodes are not shown in the photographs as they would obscure the wire array and secondary detail.

developed [9,10] to optimize the primary and secondary geometry of the system and minimize the even Legendre modes P_2 through P_8 at the capsule. Good instantaneous symmetry is obtained for secondary length and radius ($L_{\mathrm{sec}}, R_{\mathrm{sec}}$) and capsule radius ($R_{\mathrm{capsule}}$) satisfying the conditions $L_{\mathrm{sec}}/R_{\mathrm{sec}} \approx 1.3\text{–}1.7$ and $R_{\mathrm{sec}}/R_{\mathrm{capsule}} \geq 4$ [9]. Recent experiments with self-backlit foam balls have demonstrated geometric symmetry control for this system [10,11]. Odd Legendre mode asymmetry (P_1, P_3) can result from any combination of upper-lower peak pinch power mistiming, power imbalance, and pulse shape difference [3,6,9], and is a key issue for the double-ended hohlraum.

We suspend a 12 to 18 mm-long secondary in the middle of a long single array (32–38 mm), to create the two, equal-mass, equal-wire-number, 10-mm-long wire arrays above and below the secondary. Two different methods of attaching the secondary to the wire array are shown in Fig. 1. Initial scoping experiments (Fig. 1B) used glue to attach a few wires to the outer secondary wall. A more recent design for capsule implosions eliminates glue (Fig. 1C) and routes wires around a 0.5 mm raised boss on two capsule viewing apertures. The array/secondary assembly is placed within a coaxial primary hohlraum that also serves as the current return electrode for the wire array drive current (Fig. 1A). The coaxial transmission line created by the current-return electrode and the outside of the secondary feeds current to the upper array. Current flows on the lower inductance path (the outside of the secondary) and is also excluded from the inside of the secondary by the Be spokes which act as a Faraday shield. Significant current loss across the anode-cathode (AK) gap region between the two wire arrays can cause a power imbalance (smaller upper pinch power) and a mistiming of the peak pinch power (later upper wire array implosion) [6]. We have also observed sensitivity of the pinch pulse shape to aperture location and size, pinch length, AK gap size, and the wire positioning and tensioning technique [6]. Experiments with small AK-gap current loss and control of these other factors, resulting in similar upper and lower peak pinch powers and pulse shapes and thus good capsule P_1 drive symmetry, are shown in Figs. 2 and 3. The upper and lower pinch powers ($P_{\mathrm{up}}, P_{\mathrm{low}}$) and energies are measured simultaneously through 4 mm $\times$ 4 mm apertures with two sets of filtered x-ray diode arrays (XRD), and fast pulsed bolometers (BOL). The upper and lower primary hohlraum temperatures ($T_{\mathrm{up}}, T_{\mathrm{low}}$) and secondary hohlraum temperature (T_s) are measured simultaneously through (3–4)-mm-diam apertures with transmission grating spectrometers (TGS). We also use a filtered-silicon-diode array (FSDA), an imaging-silicon-diode array (ISDA), and an XRD/BOL

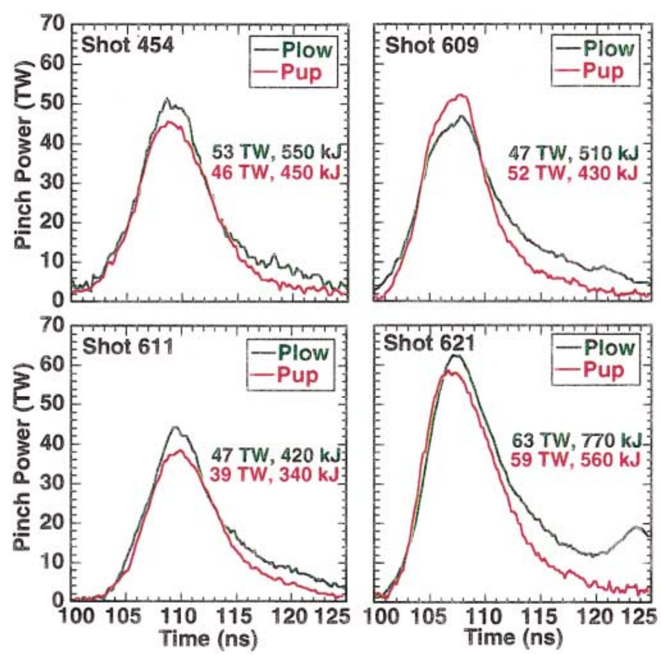

FIG. 2 (color). Upper (red) and lower (green) pinch powers for shots 454, 609, 611, 621, all in the Fig. 1B geometry, measured with x-ray diodes (XRD) and bolometers (BOL). The peak powers ($\pm 25\%$) and total energies ($\pm 15\%$) are shown on the plots.

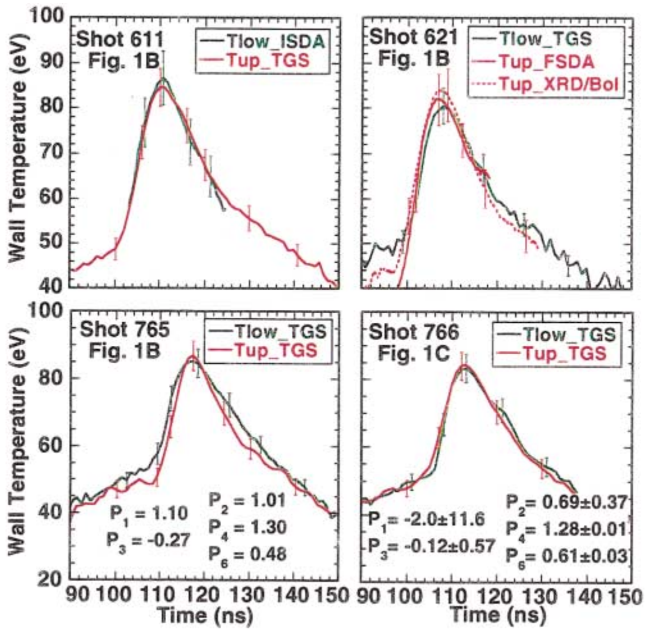

FIG. 3 (color). Upper (red) and lower (green) primary temperatures (±5%) for shots 611, 621, 765, and 766. The temperatures are labeled with the diagnostic used. Shots 611, 621, and 765 are in the array geometry of Fig. 1B. Shot 766 is in the array geometry of Fig. 1C.

combination to measure upper and lower primary temperatures. The power and temperature measurements on different lines of sight in Figs. 2 and 3 are cross timed to within ±200 ps. Aperture closure is measured with fast x-ray framing cameras.

Figure 2 shows upper and lower pinch x-ray power measurements for four shots. The average instantaneous power balance $P_{\rm up}/P_{\rm low} - 1 = -7 \pm 12\%$ at peak power. These upper and lower powers at peak are identical within the instrumental error (±25%). After peak power, however, the upper power always decreases faster than the lower in all experiments, as shown in Fig. 2. The average total radiated energy balance $E_{\rm up}/E_{\rm low} - 1 = -20 \pm 6\%$ for these shots. The lower pinch total radiated energy always exceeds the upper. The later-time upper power deficit and corresponding total energy difference may result from increasing AK-gap current loss between the two arrays after peak power. Figure 3 shows temperature measurements for the upper and lower primaries for four shots. The average instantaneous flux balance $T^4_{\rm up}/T^4_{\rm low} - 1 = 5 \pm 10\%$ at peak temperature. These peak temperatures are also identical within instrumental error (±20% in T^4). The OPTSEC model matches the measured peak primary (≈80–90 eV) and secondary temperatures (≈65–75 eV) with $\langle P_{\rm up}\rangle = 40 \pm 3$ TW, $\langle P_{\rm low}\rangle = 47 \pm 7$ TW in reasonable agreement with the average experimentally measured pinch powers of $\langle P_{\rm up}\rangle = 49 \pm 12$ TW, and $\langle P_{\rm low}\rangle = 53 \pm 13$ TW. Other hohlraum energetics models give similar results [6,7]. We have an experimental shot base of 11 shots in the scoping configuration (Fig. 1B). Of these, 40% have a peak power and temperature identical within the instrumental error, examples of which are shown in Figs. 2 and 3. However, 45% of the shots had a peak upper power more than 50% smaller than and 1 ns later than the lower, indicating AK gap current loss as the most likely explanation. The glueless implosion load design (Fig. 1C) has eliminated the shots with very large imbalance, with a 9 shot sample. This development has significantly improved our ability to perform a series of reproducible capsule implosion experiments with the double pinch.

Material ablated from the CH capsule surface by the radiation field generates an acceleration pressure on the shell related to the radiation temperature by $P \propto T^{3.5}$ [1]. A hohlraum temperature imbalance produces an asymmetrically compressed capsule that would not ignite and burn if the imbalance were too large because of mixing of colder ablator material into the hot spot. The time average of $T^{3.5}_{\rm up}(t)/T^{3.5}_{\rm low}(t) - 1$ between -5 and $+15$ ns around peak is proportional to the average P_1 capsule drive pressure imbalance. The average value of this time average for the four shots in Fig. 3 is $-2 \pm 8\%$. The OPTSEC code [9,10] was used to closely overlay measured temperature histories with predicted temperatures (e.g., see [6]) and to calculate the resultant 2D radiation field at the surface of a 2-mm-diameter capsule. The values for the time-integrated Legendre coefficients (in %) for the dominant modes are shown on Fig. 3 for 765 and 766. The time-integrated P_1 is $1.4 \pm 2.6\%$ for the measured primary temperatures averaging the four best shots. This is more than an order of magnitude less than the P_1 of 46%–49% measured in a single Z-pinch driven secondary [10,11]. Hohlraums with higher wall temperatures will have a higher albedo or wall reemission coefficient. Higher wall reradiation will smooth radiation asymmetry more efficiently. Odd Legendre mode capsule drive symmetry resulting from upper-lower pinch power imbalance (e.g., P_1, P_3) on Z (70 eV) is degraded by a factor of 1.4 relative to high yield (220 eV) because of lower wall albedo at lower hohlraum temperature. Thus these estimated P_1 levels scale to $1.0 \pm 1.9\%$ at high yield. High-yield capsule [3] sensitivity studies are underway to place limits on tolerable time-integrated P_1 capsule drive, an issue for both Z-pinch and heavy-ion-beam driven fusion. However, assuming the required P_1 is no worse than that required for P_2 suggests a $\leq 1\%$ limit [1]. The maximum possible range of uncertainty in the calculated Legendre coefficients consistent with the ±5% temperature errors is given by the cases ($T_{\rm up} + 5\%, T_{\rm low} - 5\%$) and ($T_{\rm up} - 5\%, T_{\rm low} + 5\%$) which are also given on Fig. 3 for shot 766. P_1 and P_3 are very sensitive to this error in temperature (±530%), P_2 less so (±54%). P_4 and P_6 are insensitive ($\leq \pm 5\%$). The results in Figs. 2 and 3 show the potential of this source for good instantaneous and average power balance and radiation symmetry. Direct measurements of the radiation symmetry (particularly P_1) with x-ray backlit surrogate capsules [8,12,13] are clearly required to confirm these balance measurements and symmetry models.

Figure 4 plots the average distortion from sphericity $\langle \Delta r \rangle / r$ of an imploding 2-mm-diam capsule with 60-μm-thick wall, versus the convergence ratio of the capsule gas cavity from 2D RHD [14] simulations, using the range of calculated time-dependent 2D radiation fields from shot 766. Time is implicit in these curves. Capsule distortions of $\leq$50% are required to ignite capsules ($C_r \geq 30$) in simulations considering only the effect of radiation symmetry on the implosion [1]. Distortions of $\leq$25% are recommended to provide a margin for the additional effects of Rayleigh-Taylor-induced mix of cold material into the hot spot [1]. Regions of effective radiation drive symmetry on Z that scale to these distortions at a C_r of 40 at high-yield temperature (220 eV) are also shown. Simulated capsule implosion trajectories can be approximated by a linear relationship $\langle \Delta r \rangle / r = (\langle \Delta I \rangle / I)(C_r - 1)$, where $\langle \Delta I \rangle / I$ is the effective time-averaged variation of drive intensity over the capsule surface. Capsules driven with poorer symmetry deviate from this linear relationship earlier in the implosion. The high-yield requirements ($C_r \approx 40$, $\langle \Delta r \rangle / r = 25\%-50\%$) correspond to $\langle \Delta I \rangle / I = 0.6\%-1.3\%$, respectively, for symmetry plus mix and symmetry. Even Legendre mode radiation symmetry (e.g., P_2, P_4), determined principally by hohlraum geometry, is smoothed more efficiently by wall reradiation than odd modes resulting from pinch imbalance. Even mode capsule-drive symmetry on Z is degraded by a factor of 2.8 relative to high yield because of lower wall albedo, hence these limits correspond to $\langle \Delta I \rangle / I = 1.8\%-3.6\%$. The prediction for the nominal case of shot 766 hohlraum temperature balance scales to distortions $\leq$25% at $C_r = 40$, when the increase in hohlraum wall albedo is taken into account. It should be noted that this secondary $L_{\mathrm{sec}}/R_{\mathrm{sec}}$ was not near the optimum to minimize even mode symmetry.

In conclusion, the recent double-Z-pinch progress permits the hohlraum geometry requirements of the high-yield ICF concept [3,6,7] to be fully investigated on the single-power feed Z accelerator. Despite the single-power feed, we achieved a power balance of upper and lower drives identical within the error bars on local measurements of the pinch power and primary wall temperature. A capsule C_r of at least 10 at deformations from sphericity $\langle \Delta r \rangle / r \leq 30\%$ should be possible with this source, even at the extreme limits of predicted radiation symmetry. The nominal case appears to produce radiation symmetry that scales to the requirements for high-yield capsule implosions. Direct measurements of capsule implosion quality to test these symmetry predictions are the next step [8] in our evaluation of Z-pinch technology for high-yield ICF. Capsule distortions at C_r of 5–15 can be directly measured with 4.5 to 9 keV x-ray backlighting energies produced by the Z-beamlet laser [8,10,13]. The good pinch power balance described in this Letter (which would be routinely better on a symmetric dual-power feed high-yield accelerator [3,6,7]) and the predicted scaling of odd mode symmetry, the predicted scaling of even mode symmetry for the nominal case (Fig. 4), hohlraum temperature scaling at larger pinch powers [3,6,7], the demonstrated geometric control of polar symmetry [10,11], the insensitivity of symmetry to wall motion because of large physical size and lower wall temperature compared to a laser-driven hohlraum [9,11], the expected high degree of cylindrical symmetry for Z-pinch systems [3], and the low capital cost of the technology compared to others, may well combine to offer the double-Z-pinch configuration as a future driver for high-yield ICF implosions with potential application to fusion energy.

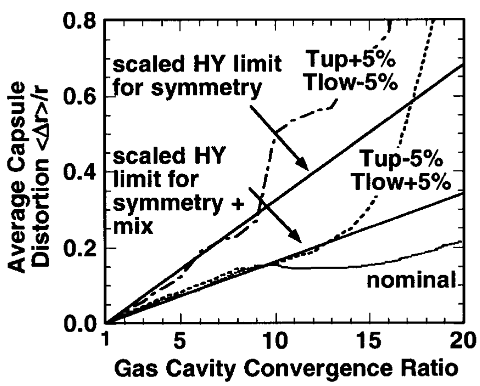

FIG. 4. Capsule average distortion from sphericity $\langle \Delta r \rangle / r$ versus gas cavity convergence ratio from 2D RHD simulations using the range of calculated time-dependent 2D radiation symmetry from OPTSEC for shot 766 in Fig. 3. Regions of capsule performance on Z that scale to high yield requirements considering symmetry ($\langle \Delta I \rangle / I = 3.6\%$) and symmetry plus mix ($\langle \Delta I \rangle / I = 1.8\%$) are also shown.

We thank J. F. Seamen and the Z accelerator operations teams for superb technical support. Sandia is a multiprogram laboratory operated by Sandia Corporation, a Lockheed Martin Company, for the U.S. Department of Energy under Contract No. DE-AC04-94AL85000.

*Electronic address: mecuneo@sandia.gov

[1] J. D. Lindl, Phys. Plasmas **2**, 3933 (1995).
[2] R. B. Spielman *et al.,* Phys. Plasmas **5**, 2105 (1998).
[3] J. H. Hammer *et al.,* Phys. Plasmas **6**, 2129 (1999).
[4] T. W. L. Sanford *et al.,* Phys. Rev. Lett. **83**, 5511 (1999).
[5] J. S. Lash *et al.,* in *Proceedings of International Fusion Science and Applications 99,* edited by C. Labaune, W. J. Hogan, and K. A. Tanaka (Elsevier, Paris, 2000), p. 583.
[6] M. E. Cuneo *et al.,* Phys. Plasmas **8**, 2257 (2001).
[7] M. E. Cuneo *et al.,* Laser Part. Beams **19**, 481 (2001).
[8] G. R. Bennett *et al.,* Bull. Am. Phys. Soc. **46**, 238 (2001).
[9] R. A. Vesey *et al.,* Bull. Am. Phys. Soc. **43**, 1903 (1998); **44**, 227 (1999); **45**, 360 (2000).
[10] R. A. Vesey *et al.,* in Proceedings of the International Conference on Fusion Science and Applications (IFSA2001), Kyoto, 2001 (to be published).
[11] D. L. Hanson *et al.,* Phys. Plasmas **9**, 2173 (2002).
[12] S. M. Pollaine *et al.,* Phys. Plasmas **8**, 2357 (2001).
[13] G. R. Bennett *et al.,* Rev. Sci. Instrum. **72**, 657 (2001).
[14] G. B. Zimmerman and W. L. Kruer, Comments Plasma Phys. Control. Fusion **2**, 51 (1975).